

PAPER • OPEN ACCESS

Development of a dynamic wake model accounting for wake advection delays and mesoscale wind transients

To cite this article: B Foloppe *et al* 2022 *J. Phys.: Conf. Ser.* **2265** 022055

View the [article online](#) for updates and enhancements.

You may also like

- [Impact of Defects in Silicon Substrate on Flash Memory Characteristics](#)
Yori Hirano, Ken Yamazaki, Fumihiko Inoue et al.
- [FLORIDyn - A dynamic and flexible framework for real-time wind farm control](#)
M Becker, D Allaerts and J W van Wingerden
- [Investigation on Evolution of Oxygen Precipitates in Bonded SOI Substrate](#)
Xin Su, Nan Gao, Meng Chen et al.



ECS Membership = Connection

ECS membership connects you to the electrochemical community:

- Facilitate your research and discovery through ECS meetings which convene scientists from around the world;
- Access professional support through your lifetime career;
- Open up mentorship opportunities across the stages of your career;
- Build relationships that nurture partnership, teamwork—and success!

Join ECS!

Visit electrochem.org/join



Development of a dynamic wake model accounting for wake advection delays and mesoscale wind transients

B Foloppe¹, W Munters¹, S Buckingham¹, L Vandeveld², J van Beeck¹

¹Environmental and Applied fluid dynamics Department, von Karman Institute, Belgium

²Electromechanical, Systems and Metal Engineering Department, Ghent University, Belgium

E-mail: benoit.foloppe@vki.ac.be

Abstract. With tip height often above 200 meters, currently installed wind turbines are increasingly interacting with the atmospheric boundary layer. Therefore, the research intends to develop a new dynamic wake model that considers weather transient inputs. The Flow Redirection and Induction in Steady State (FLORIS) framework has been proven to be a powerful wake modelling tool even though lacking dynamical effects. An extension of the FLORIS framework is presented in order to include wake advection delays between wind turbines, time-varying and spatially heterogeneous wind conditions. The so-called Observation Points (OPs) are generated at the rotor centre location. Following a Lagrangian approach, the OPs are convected downstream, along the wake of the wind turbine, defining the wake centreline. It is during this process that the dynamics of wind turbine wake and background flow field unsteadiness are included. Finally, using the same approach currently implemented for yaw-misalignment wake deflection, the wake is shifted to match the unsteady wake centreline. The developed model is validated against Large Eddy Simulation for unsteady inflow with variable wind turbine control and wake interactions. The new model is applied to a simulation of the Horns Rev wind farm with a sinusoidally time-varying wind inflow direction to show an hysteresis in the wind farm power extraction curve.

1. Introduction

Over the last decade, the size and the number of offshore Wind Turbines (WTs) and wind farms are constantly increasing and this growth is expected to continue in the future. With tip height often above 200 meters, currently installed WTs are interacting and impacting massively the atmospheric boundary layer. In the future, wind farms will become even more important contributors to the electrical power system and will require additional flexibility in terms of farm control, ancillary services and response to weather transients [1]. In this view, it is crucial for fast control-oriented models to be informed of such dynamic weather inputs. However, current models are almost always quasi-steady, hence neither exogenous nor internal wind farm dynamics are included.

Few tools are currently able to perform wake dynamics simulation while maintaining low computational cost. The FAST.Farm tool [2] is based on the Dynamic Wake Meandering (DWM) model. It is representing the dynamic wake through a collection of wake planes. The main advantages of FAST.Farm lie in the meandering feature and the coupling with FAST to model loads on wind turbines. LongSim [3] has been developed internally by DNV in order to test and evaluate wind farm control algorithms under realistic dynamic wind inflow. Gebraad and van Wingerden [4] developed the



FLORIDyn model, which is a dynamic extension of the steady-state FLORIS model [5]. Recently, a revised version of FLORIDyn was released by Becker et al. [6].

In the current work, we develop a new dynamic wake model accounting for wake advection delays and mesoscale wind transients. Similar to FLORIDyn [4, 6], this model is an unsteady extension of FLORIS, and we further refer to the model as UFLORIS. Throughout the paper, we highlight differences and similarities with the recently updated version of FLORIDyn by Becker et al. [6]. We apply the model to an idealized wind direction transient for the Horns Rev wind farm, and compare it to Large Eddy Simulation (LES) data. Section 2 outlines the methodology of extending FLORIS to include dynamic effects. Thereafter, Section 3 presents a validation study with LES data from SOWFA. Next, Section 4 discusses an application to the Horns Rev offshore wind farm subjected to a wind-direction transient. Finally, Section 5 presents the main conclusions.

2. Methodology

The Flow Redirection and Induction in Steady State (FLORIS) framework [5] has been proven to be an easy to use, easy to tune, computationally inexpensive and powerful wake modelling tool even though lacking dynamical effects. Therefore, an extension of the FLORIS framework is presented in order to include wake advection delays between wind turbines, time-varying and spatially heterogeneous wind conditions. The new dynamical model is inspired by the FLORIDyn model presented in [4] and recently revised in [6]. The so-called Observation Points (OPs) are generated at the rotor centre location as shown in Figure 1. In contrast to [6], only one OP per turbine and per time-step is created. Following a Lagrangian approach, the OPs are convected downstream, along the wake of the wind turbine, defining the wake centreline. OPs are convected with velocities computed at their current location which is another distinguishing feature from [6] where the free stream velocity (\mathbf{U}_∞) is used for every OPs. It should be stressed that both formulations are approximations and an improvement could be to use a spatial average of the disturbed (ambient plus wakes) wind velocity as proposed in [2].

In the current paper, we consider cases where the vertical OP displacement is much smaller than the horizontal displacements (computed in following LES and also shown in [7]), justifying the use of a two-dimensional dynamical model at hub height z_t . The first point of the centreline ($p = 1$), of turbine t at time step k , is located at the WT rotor centre, $\mathbf{x}_C(t) = (x_C(t), y_C(t), z_C(t))$, which gives:

$$\mathbf{x}_{t,p=1,k} = \mathbf{x}_C(t). \quad (1)$$

The downstream convection of $\mathbf{x}_{t,p,k}$ to $\mathbf{x}_{t,p+1,k+1}$ is defined as

$$\mathbf{x}_{t,p+1,k+1} = \mathbf{x}_{t,p,k} + \mathbf{U}_{t,p,k} \Delta K, \quad (2)$$

where ΔK is the time step. Thus, the previous expression can be simplified to

$$\begin{pmatrix} x_{t,p+1,k+1} \\ y_{t,p+1,k+1} \end{pmatrix} = \begin{pmatrix} x_{t,p,k} \\ y_{t,p,k} \end{pmatrix} + \begin{pmatrix} u_{t,p,k} \\ v_{t,p,k} \end{pmatrix} \Delta K. \quad (3)$$

By using matrix notation, the time update laws of OPs are:

$$\begin{bmatrix} x_{t,1,k+1} & y_{t,1,k+1} \\ x_{t,2,k+1} & y_{t,2,k+1} \\ \vdots & \vdots \\ x_{t,N_p,k+1} & y_{t,N_p,k+1} \end{bmatrix} = [A] \begin{bmatrix} x_{t,1,k} & y_{t,1,k} \\ x_{t,2,k} & y_{t,2,k} \\ \vdots & \vdots \\ x_{t,N_p,k} & y_{t,N_p,k} \end{bmatrix} + [B][x_C(t) \quad y_C(t)] + [A] \begin{bmatrix} u_{t,1,k} & v_{t,1,k} \\ u_{t,2,k} & v_{t,2,k} \\ \vdots & \vdots \\ u_{t,N_p,k} & v_{t,N_p,k} \end{bmatrix} \Delta K, \quad (4)$$

where $[A] = \begin{bmatrix} 0 & & & \\ 1 & 0 & & \\ & \ddots & \ddots & \\ \emptyset & & 1 & 0 \end{bmatrix}$, $[B] = \begin{bmatrix} 1 \\ 0 \\ \dots \\ 0 \end{bmatrix}$ and N_p is the number of OPs.

The local velocity vector $\mathbf{U}_{t,p,k} = (u_{t,p,k} \quad v_{t,p,k})$ is obtained with a steady FLORIS evaluation that reflects the background free stream velocity and turbine settings at time index k . It is important to note

that N_p is increasing at the beginning of the simulation and thus the computational time is expected to increase during the first part of the simulation and then reach a plateau.

It is during this process that the dynamics of WT wake advection delays and background flow field unsteadiness are included. Finally, using the same approach currently implemented for yaw-misalignment wake deflection, the wake is shifted to match the unsteady wake centreline. The discontinuous unsteady wake centreline deflection function is defined as

$$\delta(x_{t,p,k} - x_{t,1,k}) = (y_{t,p,k} - y_{t,1,k}), \quad (5)$$

It is representing the difference between the unsteady wake centreline and the steady wake centreline with nominal turbine settings (no yaw-misalignment).

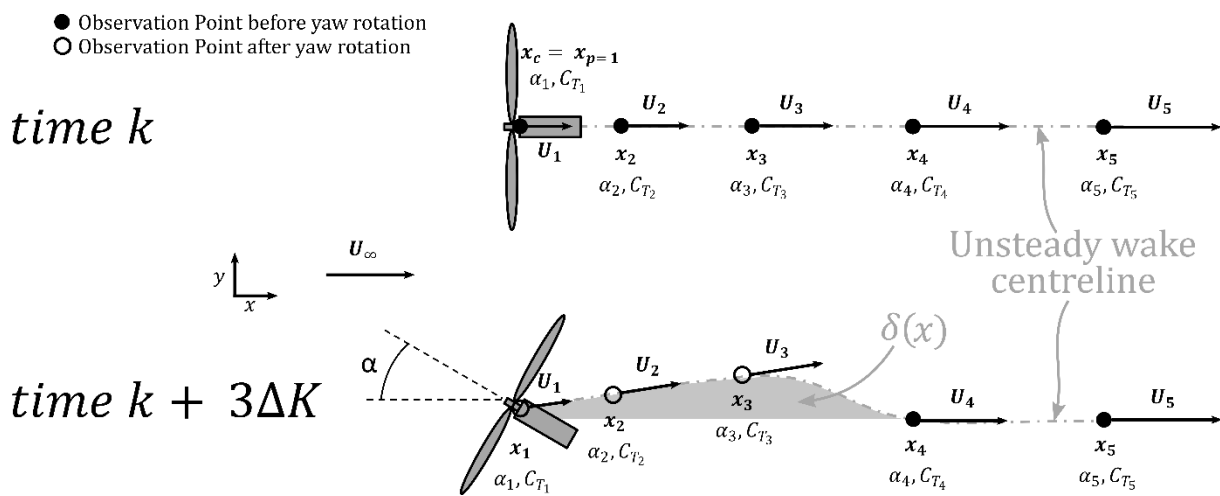


Figure 1: Illustration of the update laws, the unsteady wake centreline deflection function and the $(\alpha; C_T)$ interpolations. Since only one turbine and wake is considered, t indices are omitted in the notation.

This implementation differentiates from [4] in the fact that the original FLORIS modules, for computing wake velocity, wake turbulence and wake combination, are kept and a new module accounting for the unsteady wake centreline deflection is added. This new model can be improved by considering the variation of the yaw angle and the thrust coefficient along the wake. The α and C_T values are travelling at the same speed as the OPs. Without modifications, during the steady FLORIS evaluation of the local velocity, the current turbine settings are considered to compute the velocity deficit which is no longer correct in this unsteady approach. The velocity deficit module is updated to consider the interpolation of closest α and C_T values on the centreline as input parameters in the calculation of a local velocity inside the wake. This improvement is hereafter called “UFLORIS corrected”.

Finally, as a recap, the simulation algorithm is as follows:

1. Initialize the simulation
2. Create a new OP at the turbine location
3. Convect all OPs (Equation 4)
4. Compute current local velocities for all OPs (FLORIS call)
5. Compute the unsteady wake centreline deflection (Equation 5)
6. (optional: Compute the full 2D flow field for visualization)
7. Update time $k \rightarrow k + 1$, go to step 2.

3. Validation with LES for turbines in unsteady yaw conditions

The developed model is validated against LES by using the SOWFA tool [8]. The validation was conducted for unsteady turbulent inflow conditions, with variable WT control and wake interactions. The simulation shown in Figure 2 is set-up using 5 pairs of NREL 5MW WT represented by an actuator disk model. Turbulent inflow conditions are generated from a periodic precursor domain with dimensions of 3 x 3 kms in the horizontal directions and 1 km in the vertical direction. The resolution is 20 meters in the horizontal directions and goes gradually down to 6 meters in the vertical direction with 4 cells below the rotor and 13 cells across the rotor. The wind is coming from the bottom left at a hub-height velocity of 13 m/s and 6% of turbulence intensity. In the main simulation, the time step is 0.5s. In this simulation, the 5 upstream WTs start with a 30° yaw angle and at T=1000s the turbines start oscillating between 30° and 0° with a period of 600s during 2400s as shown in Figure 3. The WTs are spaced by 7D in downstream, x and y directions. For the UFLORIS simulation, the time step is 10s and the output flow field in Figure 2 Bottom has a resolution of 15m. The wake deficit is computed using a gaussian wake model [9]. The purpose of having 5 pairs of WTs oscillating is to be able to average the obtained results from the turbulent LES and thus obtain a more statistically relevant solution faster.

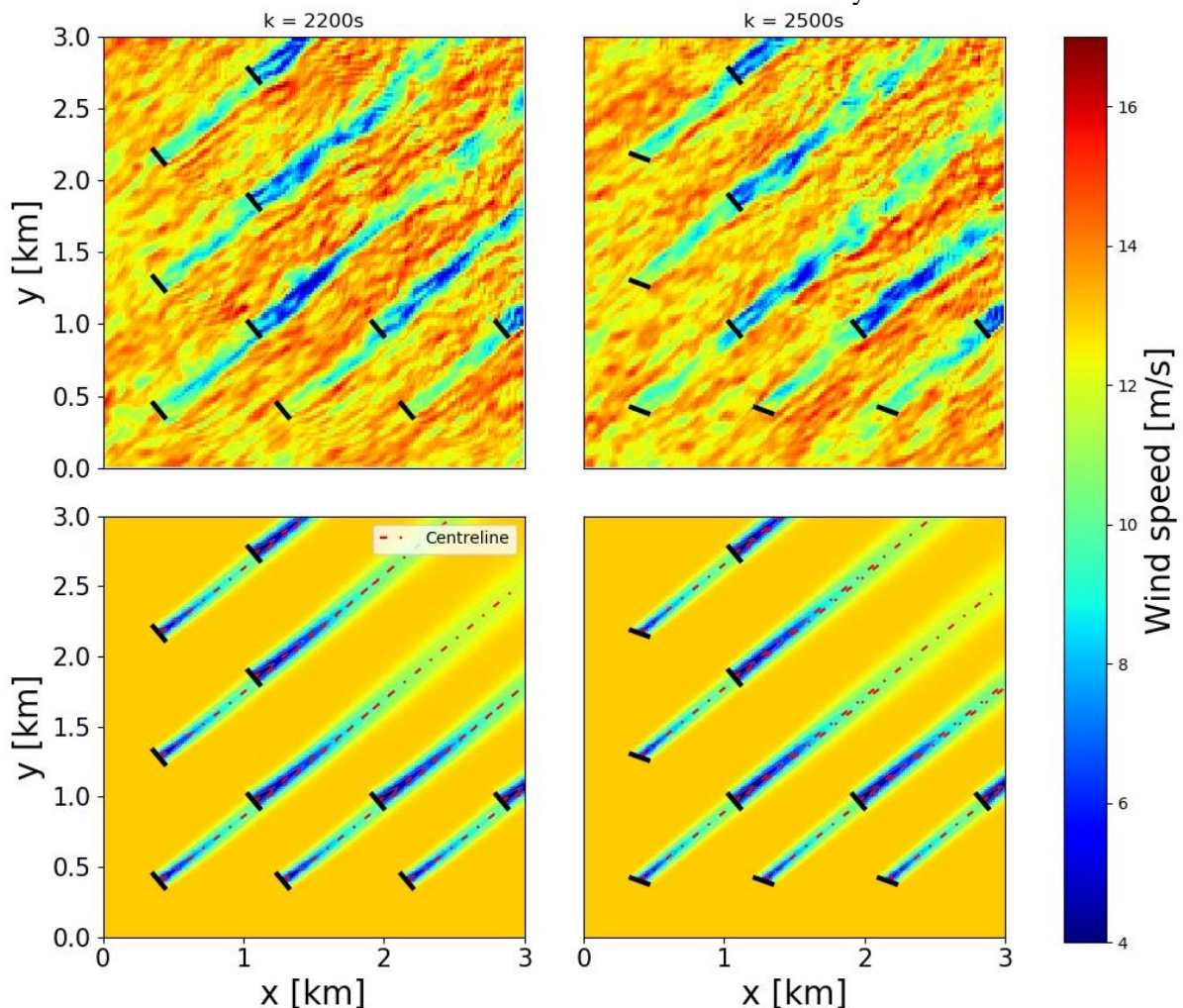


Figure 2: Contours of the instantaneous wind speed at the turbine hub height. *Left*: At $k=2200s$, $\alpha = 0^\circ$ for the front WTs. *Right*: At $k=2500s$, $\alpha = 30^\circ$ for the front WTs. *Top*: SOWFA. *Bottom*: UFLORIS.

Figure 2 is showing the comparison between the SOWFA simulation (Top) and the corresponding UFLORIS simulation (Bottom). In the UFLORIS simulation, the turbulence is only considered to compute the wake deficit hence the free stream is set to 13 m/s. Left figures are showing contours of the instantaneous wind speed at the turbine hub height when upstream WTs are facing the wind. In right figures, WTs are experiencing a yaw-misalignment of 30° . The velocity deficit from the UFLORIS is comparing well with the SOWFA results when looking at downstream WT wakes. Bottom figures are also displaying the unsteady wake centrelines for every WT. It can be noticed that when $\alpha = 0^\circ$, the wake centreline is crossing the downstream turbine rotor in the right part. However, when $\alpha = 30^\circ$, the wake centreline is crossing the downstream turbine rotor near the middle. It would be the opposite at steady state. This is showing that the delay between a change in WT setting and its impact on the downstream WT is correctly captured by UFLORIS.

Figure 3 is presenting the averaged power of the five downstream WTs as a function of time (Top). The SOWFA results are filtered with a moving average of 3 minutes in order to remove turbulent fluctuations and facilitate the comparison. On top of the UFLORIS and UFLORIS corrected versions described before, the Quasy-Steady FLORIS (QS FLORIS) simulation is added. It is basically a collection of steady-state computations with varying turbine settings. Therefore, the QS FLORIS power is exactly in phase with the upstream turbine yaw angle. The two UFLORIS simulations show a delay between the change of the yaw angle and its impact on the power. The results are significantly improved compared to QS FLORIS and reducing the absolute error with the filtered SOWFA power (Bottom). The corrected version is located between the black and the red dashed curves as expected. In fact, the decrease in yaw angle is slowing down the convection of OPs. In the uncorrected version, all OPs are instantaneously affected by the change of yaw because there is only one yaw angle parameter for the whole wake. This is leading to a slower displacement of the unsteady wake centreline and then a delayed full wake interaction configuration. In this case, the corrected version is not improving the results but it should be stressed that both UFLORIS simulations are showing a small phase shift compared to the SOWFA power. One possible explanation is the lack of axial induction effect in the wake deficit computation. The axial induction is slowing down the wind upstream of the wind turbine and thus delaying the full wake interaction configuration.

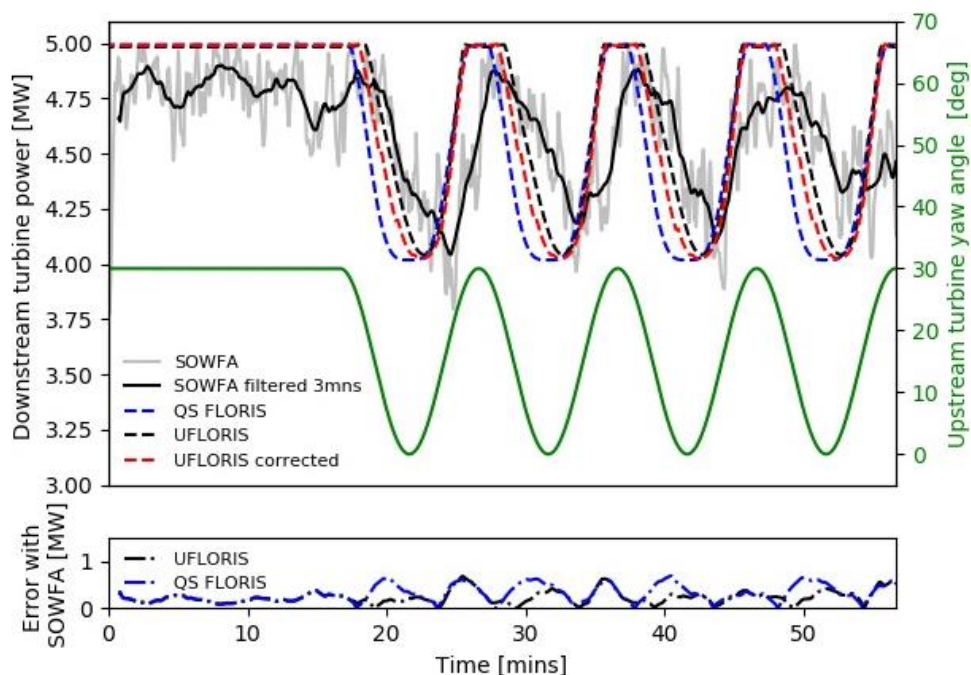


Figure 3: *Top*: Averaged downstream WT power comparison and upstream WT yaw angle. *Bottom*: Absolute errors with SOWFA filtered.

Figure 4 presents a phase-averaged result over each oscillation period. The new red solid line is corresponding to the average of the SOWFA filtered curve in Figure 3. This Figure is also showing that the decrease period is taking more time than the increase (2/3 of the period). It is corresponding to the slowdown of the incoming OPs generated with lower yaw angle. This dynamic behaviour is also observed in both UFLORIS simulations. Note that the discontinuities in the UFLORIS corrected curve are caused by the large time step.

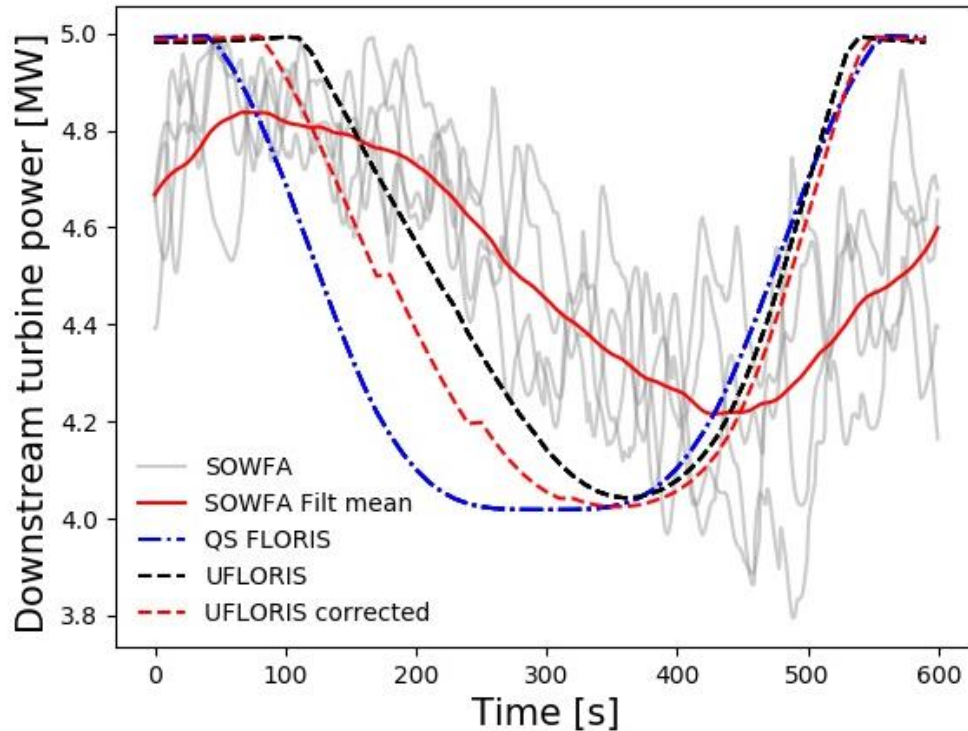


Figure 4: Averaged downstream WT power comparison for the four 600s-periods.

4. Application to Horns Rev subjected to a wind-direction transient

4.1. Mesoscale wind-direction transient

The UFLORIS model is used to simulate the Horns Rev wind farm consisting of 80 Vestas V80-2MW turbines in a rhomboid layout (see Figure 5). A sinusoidally time-varying wind inflow direction ($\theta(k) = 270^\circ - 30^\circ \sin(2\pi k/T_\theta)$) is applied. The wind is coming from the left at a magnitude of 8 m/s at hub height and around 7.5% of turbulence intensity. The wind direction is oscillating between 240° and 300° while the WT are always facing the wind (no yaw-misalignment). In this first case, the change in wind direction is applied uniformly across the domain, representing a wind direction change generated by a very large-scale effect (or mesoscale effect). It is an ideal test-case to assess this new dynamical wake model because it involves dynamics of wake advection delays in wind farms and dynamical hysteresis effects in power production as shown by LES results in [10].

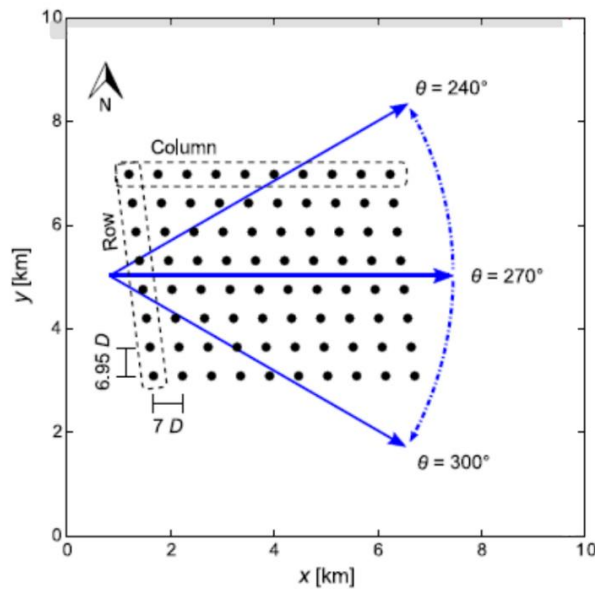


Figure 5: Layout of the Horns Rev wind farm [10].

In Figure 6, results are compared with LES from [10] for three different periods of oscillation ($T_\theta = 1h, 2h, 4h$). First of all, UFLORIS is capable of capturing the power hysteresis in the normalized power curve for both shorter periods. For $T_\theta = 4h$, UFLORIS is still capturing an hysteresis while it is not evident in the LES. As expected, results are converging to the steady state solution when the rate of oscillation is decreased. It can be noticed that the starting wind direction is 270° and thus the red curves are starting from the steady state value and then reaching the other unsteady curves. Unlike the LES results, UFLORIS results are not going lower than FLORIS minimum value. Munters et al. hypothesize this effect is due to high-speed channels in between turbine columns in LES steady wind direction simulation [10], an effect which is not captured in our simple wake model. Due to this difference in the steady-state wind farm power between UFLORIS and LES at 270° , the normalization of the UFLORIS results is done with LES at $\theta = 240^\circ$. Except for three steady state values around 270° , FLORIS is comparing well with LES. On top of a good estimation of the power minimum locations, UFLORIS is showing good agreement with LES to represent small power variations apart from the middle region ($240 < \theta < 260$ and $280 < \theta < 300$). This shows the high potential of UFLORIS to represent wake dynamic behaviours.

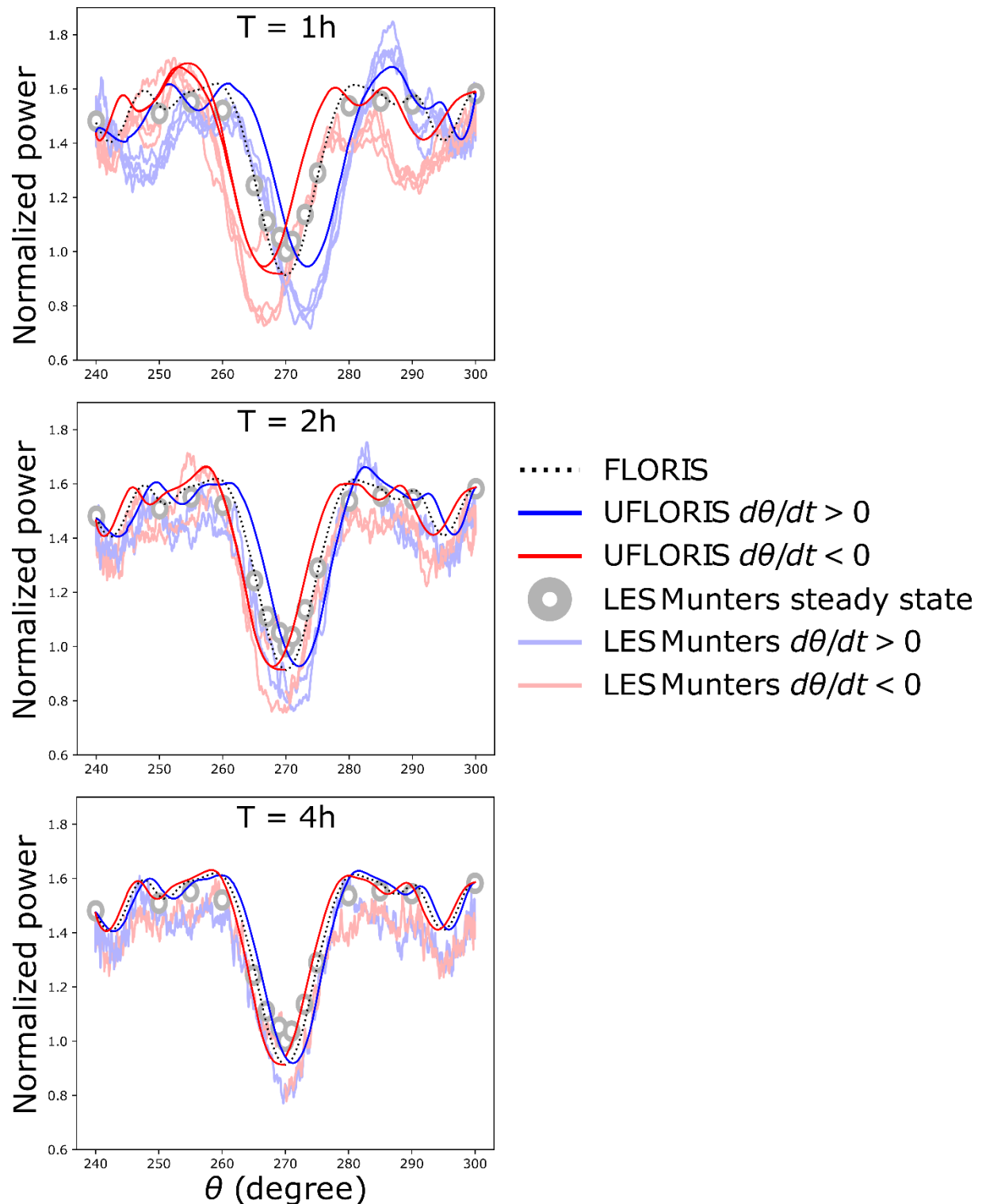


Figure 6: Horns Rev wind farm power variations as a function of wind directions for 3 different oscillation period: $T_\theta = 1h$ (Left), $2h$ (Middle), $4h$ (Right). Powers are normalized with steady-state power in LES for $\theta = 240^\circ$. Opaque lines indicate (U)FLORIS results produced in the current paper. Transparent lines are LES results from Munters et al. [10]

4.2. Frontal wind-direction transient

In order to investigate the potential usage of an unsteady wake model, a new type of wind direction change is investigated. While before the wind direction was changing everywhere at the same time, now the wind direction is propagating inside the wind farm. This is representing a small atmospheric-scale effect like a frontal wind passage or a storm. The wind direction is still oscillating as previously defined but it is now corresponding only to the value of the WT at the North-West corner. Then the change propagates through the wind farm at the free-stream velocity of 8 m/s. For this case, the UFLORIS model is not necessary as the heterogenous wind direction can be directly incorporated into the free stream flow field with FLORIS. Thus, frontal direction change is comparable to a QS FLORIS simulation.

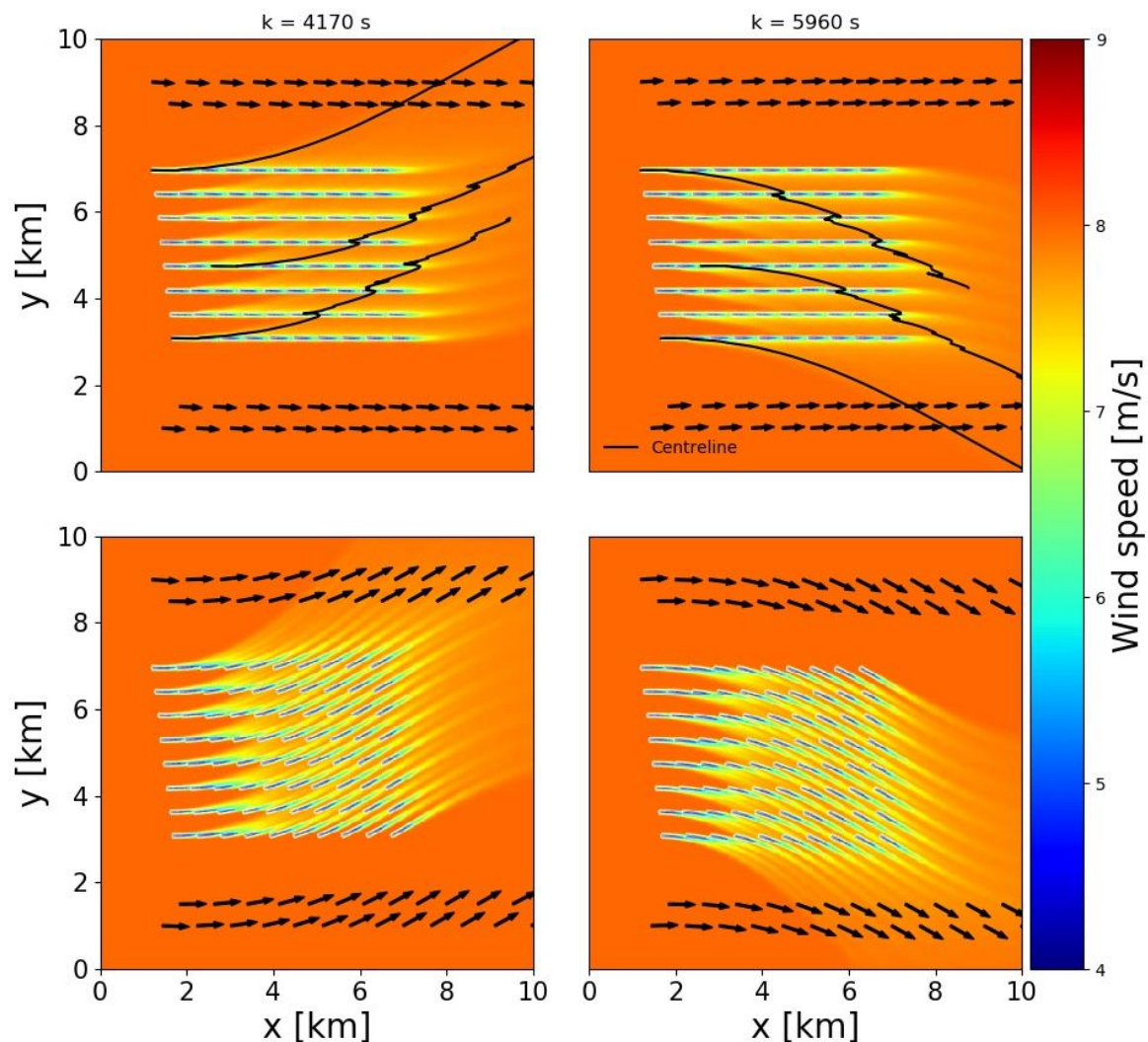


Figure 7: Contours of the instantaneous wind speed at the turbine hub height. *Left*: At $k=4170$ s, $\theta = 273.6^\circ$. *Right*: At $k=3660$ s, $\theta = 266.7^\circ$. *Top*: Mesoscale wind direction change. *Bottom*: Frontal wind direction change.

In Figure 7, a comparison between the mesoscale (Top) and frontal (Bottom) wind direction definitions is shown for two different time steps corresponding to the minima of UFLORIS in Figure 6 Left: $\theta = 273.6^\circ$ at $k = 1870$ s (Left) and $\theta = 266.7^\circ$ at $k = 3660$ s (Right). The same period of $T_\theta = 1$ h is used. The arrows are representing local wind directions. For Top figures, only three unsteady wake

centrelines are represented in order to avoid overload of the figure but every WT as an associated centreline. It can be seen that the two wind direction change formulations are leading to very different wake deviations inside the wind farm. In the frontal wind figures, WTs on the West part are largely interacting while on the East they are not. Because of this fast wind direction change, strong wake interactions are always limited to subsets of wind turbines, and are rarely present in the entire farm leading to a flatter power curve as shown in Figure 8 blue curve. Figure 8 is also showing that when the rate of oscillation is decreased, frontal results are converging to the steady state solution. Finally, with a period of 4h, the frontal formulation is similar to the mesoscale formulation with a period of 1h.

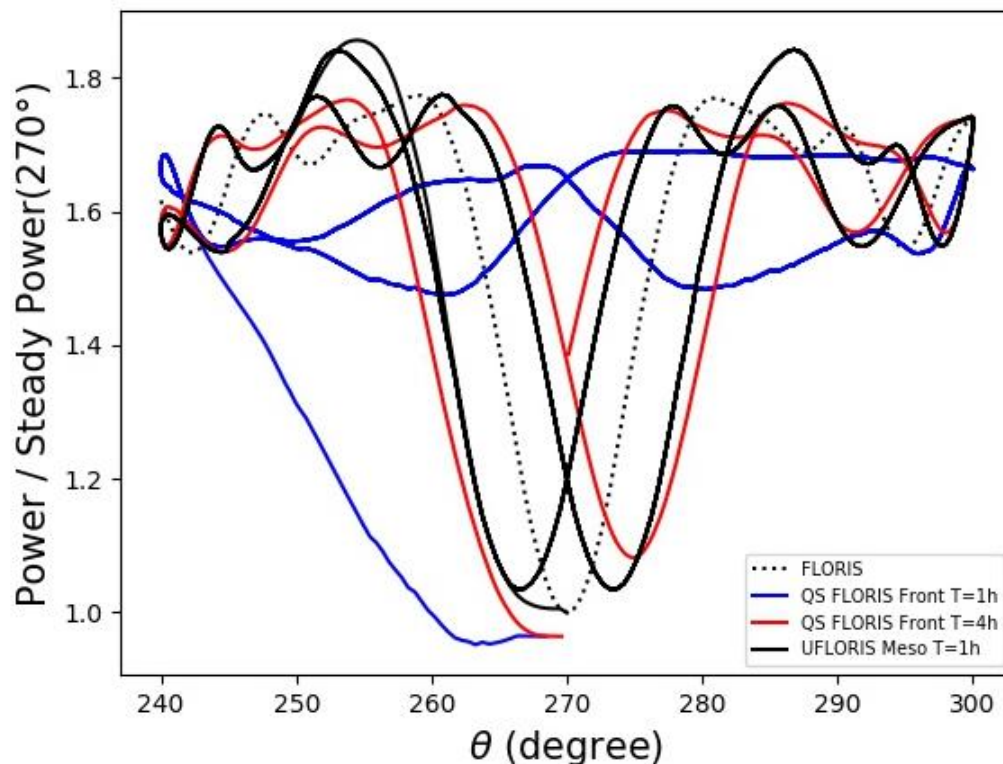


Figure 8: Power variations as a function of wind directions for mesoscale and frontal wind direction change formulations.

5. Conclusions

In order to consider wake advection delays and mesoscale wind transients, dynamic wake models are necessary. In this paper, the development of a dynamic wake model is presented and corresponds to a dynamic extension of the steady-state FLORIS. Differences with similar models have been highlighted showing the originality of UFLORIS. Both the validation and the application show the high potential of UFLORIS to represent wake dynamic behaviours. Comparison with LES over the Horns Rev wind farm shows that this new model is able to capture predominant unsteady wake effects but also fine details. Unsteady wake models are opening new possibilities for engineering applications like operational power forecast. Coupled with a weather prediction model, it would be possible to estimate wind-power resources accounting for the influence of synoptic phenomena or to improve current wind farm parametrizations that are commonly used at mesoscale level by informing on sub-grid scale effects. A stand-alone usage is also possible where the flow field is derived from a single measurement location.

Acknowledgements

The authors acknowledge support from the PhairywinD project, funded by the Energy Transition Fund of the Belgian Federal Public Service for Economy, SMEs, and Energy (FOD Economie, KMOs en Energie).

References

- [1] Eguinoa I, Göçmen T, Garcia-Rosa PB, Das K, Petrović V, Kölle K, Manjock A, Koivisto MJ and Smailes M 2021 Wind farm flow control oriented to electricity markets and grid integration: Initial perspective analysis *Advanced Control for Applications* **3(3)**
- [2] Jonkman JM, Annoni J, Hayman G, Jonkman B and Purkayastha A 2017 Development of FAST.Farm: A New Multi-Physics Engineering Tool for Wind-Farm Design and Analysis *35th Wind Energy Symp. (Grapevine Texas : SciTech) Preprint*
- [3] E. Bossanyi et al. 2018 Description of the reference and the control-oriented wind farm models, CL-Windcon deliverable D1.2 Available at: <https://ec.europa.eu/research/participants/documents/downloadPublic?documentIds=080166e5ba664d11&appId=PPGMS>.
- [4] Gebraad PMO and van Wingerden JW 2014 A Control-Oriented Dynamic Model for Wakes in Wind Plants *J. Phys.: Conf. Series* **524** 012186.
- [5] 2021 FLORIS Version 2.4 Available at <https://github.com/NREL/floris>.
- [6] Becker M, Ritter B, Doekemeijer B, van der Hoek D, Konigorski U, Allaerts D and van Wingerden JW 2022 The revised FLORIDyn model: Implementation of heterogeneous flow and the Gaussian wake *Wind Energy Science Discussions Preprint*
- [7] Bossuyt J, Scott R, Ali N and Cal RB 2021 Quantification of wake shape modulation and deflection for tilt and yaw misaligned wind turbines *Journal of Fluid Mechanics* **917**.
- [8] Sale D, Churchfield M and Bachant P 2020 dcsale/SOWFA: v1 *Zenodo* Available at <https://doi.org/10.5281/zenodo.3632051>.
- [9] Bastankhah M and Porté-Agel F 2014 A new analytical model for wind-turbine wakes *Renewable Energy* **70** 116–123.
- [10] Munters W, Meneveau C and Meyers J 2016 Turbulent Inflow Precursor Method with Time-Varying Direction for Large-Eddy Simulations and Applications to Wind Farms *Boundary-Layer Meteorology* **159.2** 305–328.